Supramolecular Chemistry
Publication details, including instructions for authors and subscription information:
http://www.informaworld.com/smpp/title~content=t713649759

Complex Formation of Some Tetraamido-type Calix[4]arene Derivatives Detected by Vibrational Spectroscopy

Ildikó Mohammed-Ziegler[a]; Abdelwaheb Hamdi[b]; Rym Abidi[b]; Jacques Vincens[c]
[a] IR and Raman Laboratory, Chemical Research Center of the Hungarian Academy of Sciences, Budapest, Hungary [b] Facultés des Sciences, Université de Bizerte, Tunis, Tunisie [c] Ecole Chimie Polymères Materiaux, Laboratoire de Conception Moléculaire, Strasbourg, Cedex 2, France

To cite this Article Mohammed-Ziegler, Ildikó , Hamdi, Abdelwaheb , Abidi, Rym and Vincens, Jacques(2006) 'Complex Formation of Some Tetraamido-type Calix[4]arene Derivatives Detected by Vibrational Spectroscopy', Supramolecular Chemistry, 18: 3, 219 — 234
To link to this Article: DOI: 10.1080/10610270500485214
URL: http://dx.doi.org/10.1080/10610270500485214

Supramolecular Chemistry, April–May 2006 Vol. 18 (3), pp. 219–234

Complex Formation of Some Tetraamido-type Calix[4]arene Derivatives Detected by Vibrational Spectroscopy

ILDIKÓ MOHAMMED-ZIEGLER[a,*], ABDELWAHEB HAMDI[b], RYM ABIDI[b] and JACQUES VINCENS[c]

[a]*IR and Raman Laboratory, Chemical Research Center of the Hungarian Academy of Sciences, Pusztaszeri út 59-67, H-1025 Budapest, Hungary;* [b]*Facultés des Sciences, Université de Bizerte, 7021 Zarzouna-Bizerte, Tunis, Tunisie;* [c]*Ecole Chimie Polymères Materiaux, Laboratoire de Conception Moléculaire, associé au CNRS, 25 rue Becquerel, F-67087 Strasbourg, Cedex 2, France*

Received (in Southampton, UK) 22 July 2005; Accepted 22 November 2005

Complex formation of five teraamido-type calix [4] arene derivatives—containing a heteroaromatic ring on the carboxamide moieties forming the coordination sphere—with alkali/alkali earth ions were the subject of FT–IR studies. The selectivity of these ligands toward different cations were found in acetonitrile solution, with the best detection in the case of the thiophene derivative, ligand 3, that exhibited selectivity to thallium(I) and thallium(III) ions over alkali/alkaline earth ions. Calixarenes 2 and 4 exhibit selectivity to potassium and ligand 5 to lithium ions among alkali/alkaline earth ions, however, thallium(I) ions show interference with these measurements. Moreover, selectivity was observed in solid state when surface complexes were prepared on sodium chloride, potassium chloride, bromide and iodide, calcium chloride and fluoride. The solid samples were examined by FT–Raman and Diffuse Reflectance Infrared Fourier Transform Spectroscopy (DRIFTS) method. Calixarenes 2 and 4 are of potential analytical application for the recognition of cations among alkali/alkaline earth metal ions in solid state by FT–IR spectroscopic detection. The number of methylene units in the substituents of calixarenes influences the efficiency of the complexation process significantly, as it can be seen from the comparison of ligands 1 and 2 both in solution and in the solid state. FT–Raman measurements on calcium chloride show that the attachment of the ligand molecules to the salt surface is accompanied by the squeezing of water molecules from some special positions of the hydrated salt lattice.

Keywords: Calix[4]arene; Alkaline/alkaline earth ions; Complex, FT–IR; FT–Raman

INTRODUCTION

Calixarenes are cyclic oligomers exhibiting molecular recognition properties [1]. They aroused much attention in the recent decades due to their ability to chelate ions or aliphatic amines selectively [2–4] therefore much effort has been concentrated to apply calixarenes as active components of electrochemical and/or optical sensors (optrodes) [5–8]. Calixarene derivatives also exhibit host-guest interactions with neutral molecules [9,10].

FT–IR spectroscopy is efficient to observe host-guest interactions in macrocycles such as β-cyclodextrin [11,12], crown ether derivatives [13–15] and calixarenes [14–17]. As it is known, the analysis of the IR spectra of such molecules is a rather difficult task since their great size results in very complex vibrational spectra. The full assignment of tetrahydroxy-calix[4]arene based on *ab initio* calculations has recently been presented by Billes and Mohammed-Ziegler [18].

In the present work, the complex formation of ligands **1–5** with different metal ions is investigated by means of FT–IR spectroscopy, their general structure is presented in Fig. 1. The four benzene rings constitute a conical skeleton to which four heterocyclic moieties are attached via aminocarbonylmethoxy bridges on the lower rim in order to form a complexation sphere.

Preliminary studies have already been performed on the complex forming behaviour and selectivity of calixarenes **1–5** with alkali, alkaline earth and zinc ions by ^{1}H NMR spectroscopy [19]. It was found that these ligands are all able to form complexes both with one or two lithium ions in chloroform-d depending on the molar ratio of the reactants. However, only ligand **4** can form complexes with

---

*Corresponding author. E-mail: mohazihu@yahoo.com. Present address: Gedeon Richter, Ltd, Quality Control, Department, Esztergomi út 27., H-2510, Dorog, Hungary.

ISSN 1061-0278 print/ISSN 1029-0478 online © 2006 Taylor & Francis
DOI: 10.1080/10610270500485214

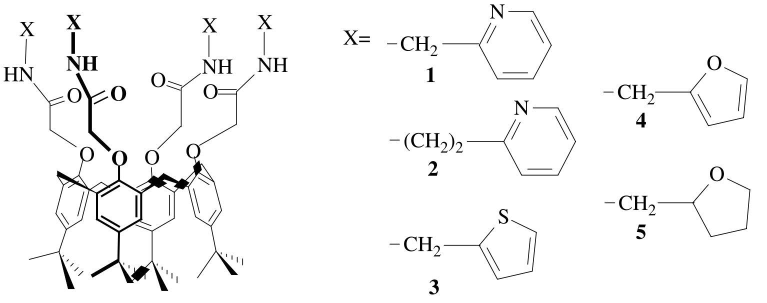

FIGURE 1 Chemical structure of calixarenes **1**–**5**.

sodium ions characterized by both 1:1 and 1:2 stoichiometries in case of the proper composition of the system. Calixarenes **1**–**4** chelate sodium only as 1:1 complexes, whereas a lithium ion can be chelated by the stoichiometry 1:1 and 1:2. Moreover, ligands **1** and **2** were ready to form complexes with zinc ions [19].

The aim of the present study was to apply FT–IR spectroscopic detection in order to obtain more sensitive differentiation between ions than with, e.g. UV/Vis spectroscopy and evaluate the results from the point of view of potential analytical application of the studied ligands. The complexation of metal cations were unambignously demonstrated. Differences in the structure of complexes formed in solution and on the surface of solid salts have been investigated.

EXPERIMENTAL SECTION

Chemicals

Sodium chloride (Suprapure®, >99.99%), potassium chloride (>99.5%), potassium bromide (Uvasol®), potassium iodide (>99.5%), anhydrous calcium chloride (>90%), calcium fluoride (Suprapure®, >99.95%), and thallium(III) chloride (pro analysi) were purchased from Merck. Acetonitrile (LiChrosolv®, >99.9%) and chloroform (>99%) were also the product of Merck. Thallium(I) chloride (>99%) and lithium chloride (>99.9%), were supplied by Aldrich.

For FT–IR experiments, saturated acetonitrile solutions of ligands **1**–**5** were prepared (separately), in which one of the aforementioned salts was dissolved and the spectra were recorded within a few minutes.

Transmission spectra of the samples (0.505 mm layer thickness) were recorded in a NaCl liquid cell relative to a NaCl crystal possessing identical window thickness. Spectra were obtained on a Nicolet Magna 750 FT–IR instrument at a resolution of 4 cm^{-1}; 128 scans were accumulated. The curve fitting of ν(C=O) vibrational band contours were carried out by the software PCCAP (by J. Varga and J. Lejtovicz, 1991).

Prior to Diffuse Reflectance Infrared Fourier Transform Spectroscopy (DRIFTS) measurements, the salts were dried at 110°C for five hours and then stored in a desiccator until the experiment. Samples were prepared by adding 1 ml of chloroform stock solution (0.6 g/l) of each ligand to 0.04 g of salt, air dried and then dried at 60°C for two hours. DRIFT spectra of the solid samples were acquired on a Perkin Elmer System 2000 FT–IR instrument equipped with a Perkin Elmer Diffuse Reflection Accessory. For each sample, 256 scans were accumulated at a resolution of 1 cm^{-1}. Alkali halogenide salts are known as good optical windows in the mid-IR region, thus they behave as transparent scattering matrices, and therefore were used in neat form as reference while recording the DRIFT spectra. The processing of the data was as follows: the spectrum of the water vapour was subtracted from every sample spectrum, and then 7-pont-smoothing was carried out. Data were processed by using the Nicolet Omnic software.

Raman spectra were measured on a Perkin Elmer System 1760X FT–IR instrument equipped with a 1700X Raman supplement. The samples were excited with the intensity-stabilized 1064 nm radiation from a Spectron SL 301 Series Nd:YAG laser at 0.8 W (deviations from the 0.8 W of laser power are noted in the text). A total of four hundred scans were accumulated to achieve good signal-to-noise ratio. The same samples were used for recording the Raman spectra as for the measurement of the FT–IR spectra. The processing of the data was performed by subtracting the Raman spectrum of the corresponding neat salt from the sample spectrum, and then a 7-point-smoothing was applied to the difference spectra.

RESULTS AND DISCUSSION

The complexity of the FTIR spectra of calixarene derivatives is illustrated in Fig. 2. Here, the spectra of chloroform solution of the ligands **1**–**5** are shown, and the location of major bands are also indicated on the graph. As expected, these spectra

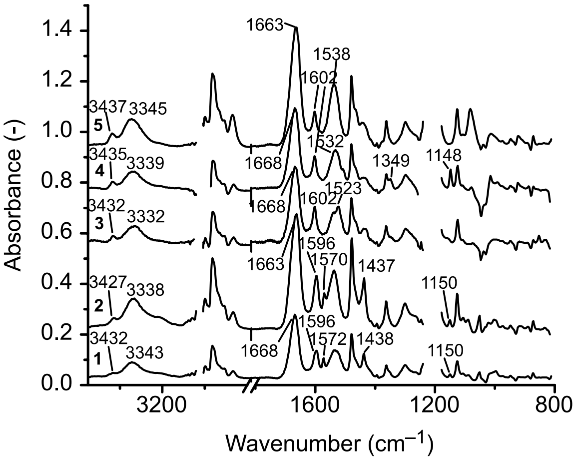

FIGURE 2 The IR spectrum of calixarenes **1**–**5** in chloroform solution measured in a NaCl liquid cell (the chloroform bands are compensated) with a tentative assignment of the most intense bands; spectra of ligands **2**–**5** are off-set for clarity.

are rather similar. However, characteristic spectral differences are also observed as a consequence of the different heteroaromatic substituents in the coordination spheres of ligands **1–5** (Fig. 1). The location and tentative assignment of the most characteristic vibrational bands are summarized in Table I.

Bands corresponding to the calixarene skeleton can be easily assigned based on earlier experience [21], additionally, the amide ν(NH), hydroxyl stretching {ν(OH)}, the amide-I vibrational modes and the aromatic stretching modes of the calixarene skeleton {$\nu(CC)_{rg}$}. The ligand molecules themselves do not contain any hydroxyl groups, however; the ν(OH) bands are always clearly detected and they probably correspond to water traces present in the solutions. Under the title "other vibrational bands" those specific bands are listed that correspond to the heterocyclic substituents. It is remarkable that the tetrahydrofuranyl moiety does not exhibit indicative vibrations and/or vibrations that can form a base for differentiating between the studied ligands. Probably, it is due to the fact that the ring vibrational modes overlap with those of the calixarene skeleton and therefore they are not discernible.

Complex Formation in Solution

Complex formation of ligands **1–5** with various cations were studied in acetonitrile solutions. The poor solubility of the studied ligands in acetonitrile prevented us from measuring their infrared spectra in this solvent with good signal-to-noise ratio. However, the complex formation causes such structural changes that the complexes formed are conveniently observable in acetonitrile whereas they cannot be studied in chloroform since metal chlorides are poorly soluble in this solvent.

The amide-I region of calixarene **1** is shown in Fig. 3a in the presence and in the absence of different metal halogenides. It is important to note that conclusions have to be drawn carefully during the analysis of these spectra because the location of the deformation vibration of water (at around 1630 cm^{-1} as revealed from an independent measurement) is also in the vicinity of the carbonyl modes of calixarenes **1–5**, and thus the superimposed spectra of the bands are recorded. As can be seen, the envelopes are quite similar and the deviation between the spectra is not sufficient to establish a base for the differentiation between the cations, e.g. in a mixture where the concentration of the ions ought to be measured.

The spectral changes of the FT–IR spectra of ligand **2** are illustrated in Fig. 3b in the presence and in the absence of different metal halogenides. In this paper, our attention was focused mainly on the amide-I vibrations and the specific modes of the heteroaromatic rings, since the corresponding moieties form the coordination sphere of the ligands under study (see Fig. 1). Coordination of the added ions cause the change of the chemical surrounding of the aforementioned amide-I vibrations and the specific modes of the heteroaromatic rings and thus spectral changes, i.e. shifts of the bands and sometimes their broadening are observed directly.

As apparent, the insertion of an additional methylene moiety in the "arms" of the complexation sphere (see Fig. 1) increases somewhat the selectivity of the studied ligand with respect to calixarene **1** in acetonitrile solution. Potassium can be selectively detected among alkali ions. Thallium(I) also tends to form complex readily with ligand **2**, however, the simultaneous presence of potassium ions disturbed the measurement.

As can be seen from Fig. 4., calixarene **3** exhibits selectivity to thallium ions over alkali/alkaline earth ions. Thallium complex may be detected on the basis of the band centered at 1691 cm^{-1}, however, complex is formed without respect to the charge number of the thallium ion. The simultaneous presence of lithium ions may cause interference during a measurement of thallium concentration.

As shown in Fig. 5a, calixarene **4** exhibits selectivity to potassium ions among alkali/alkaline earth ions, however, the presence of thallium(I) ions cause error in the measurement. Calixarene **5** (see Fig. 5b) is selective to lithium ions over alkali/alkaline earth ions, but similarly to ligand **4**, thallium(I) may interfere the determination.

It is important to underline that the solvent acetonitrile cover up a noticeable part of the mid-IR region that can lead to the failure of the detection of some spectral changes caused by complex formation. However, the solubility requirements reduce significantly the number of potential solvents in this study.

TABLE I Selected vibrations in the infrared spectra of chloroform solution of calixarenes **1**–**5** (sh denotes shoulder, the assignments are based on the literature written below, for explanation of the symbols see [20]).

Assignment and literature	**1**	**2**	**3**	**4**	**5**
	Location (cm^{-1})				
ν(NH) and	3432	3427	3432	3435	3437
ν(OH) [21]	3343	3338	3332	3339	3345
Amide-I [21]	1668	1663	1668	1668	1663
$\nu(CC)_{rg}$ [18,21,29]	~1602 sh	~1602 sh	1602	1602	1602
Other vibrational bands	1596 $\nu(CC)_{pyr} + \nu(CN)_{pyr}$ [30]	1596 $\nu(CC)_{pyr} + \nu(CN)_{pyr}$ [30]			
	1572 $\nu(CC)_{pyr} + \beta CC)_{pyr}$ [30]	1570 $\nu(CC)_{pyr} + \beta(CC)_{pyr}$ [30]	–	–	–
	1533	1537	1540 $\nu(CC)_{tio} + \delta(CH)_{tio}$ [28]	1532 $\nu(CC)_{fur} + \beta(CH)_{fur}$ [27]	1538 $\gamma(CH)_{thf}$ [27]
			1523 $\nu(CC)_{tio} + \delta(CH)_{tio}$ [28]		
	1438 $\beta(CH)_{pyr} + \delta(CC)_{pyr}$ [30]	1437 $\beta(CH)_{pyr} + \delta(CC)_{pyr}$ [30]	–	–	–
	–	–	~1349 sh $\delta(CH)_{tio} + \nu(CC)_{tio}$ [28] or $\nu(CC)_{tio}$ [25]	1349 $\nu(CC)_{fur} + \beta(CH)_{fur}$ [27]	–
	1150 $\delta(CH)_{pyr} + \nu(CC)_{pyr} + \nu(CN)_{pyr}$ [30]	1150 $\delta(CH)_{pyr} + \nu(CC)_{pyr} + \nu(CN)_{pyr}$ [30]	~1148 sh $\nu(CC)_{tio}$ [25] (based on 2,2′-bithiophene)	1148 $\beta(CH)_{fur} + \nu(CO)_{fur+}\nu(CC)_{fur}$ [27]	–
	–	–	~702 $\gamma(CH)_{tio}$ [26,28]	–	–
	613 $\beta(CC)_{pyr} + \delta(CN)_{pyr}$ [30]	615 $\beta(CC)_{pyr} + \delta(CN)_{pyr}$ [30]	–	–	–
	–	–	–	599 $\gamma(CH)_{fur}$ [27]	–

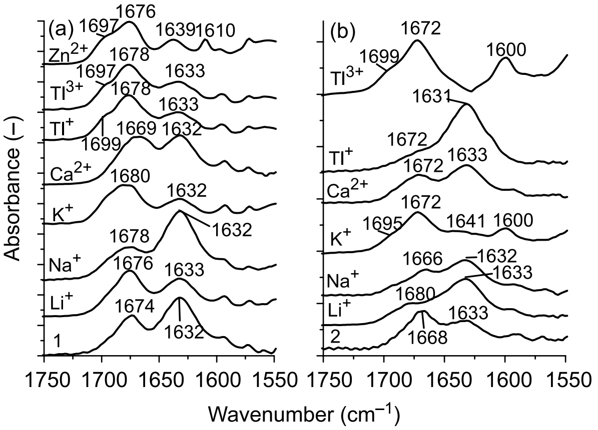

FIGURE 3 The amide-I region of the IR spectra of calixarenes **1** (a) and **2** (b) in the presence and in the absence of some metal halogenides in acetonitrile solutions. Cations are indicated on the graphs.

It is likely that the complex formation cause different spectral changes in the FTIR spectra because alkali/alkaline earth ions and heavy metal ions are coordinated at different locations of the ligands, i.e. heavy metal ions are coordinated by the heteroaromatic rings, whereas alkali/alkaline earth ions are by the C=O moiety of the amide groups and the phenolic oxygen of the calixarene skeleton (see also [6]). This assumption is supported by the preliminary NMR results [19].

Formation of Surface Complexes

DRIFTS Experiments

For comparison, the DRIFT spectra of the pure ligands **1–5** recorded in KBr matrix are shown in Fig. 6. The most relevant changes in the spectra are discussed here in comparison with the results of the solution experiments. First of all, the N—H stretching vibrations are shifted to lower wavenumbers, and thus they are detected as shoulders in solid state, the O—H stretching vibrations are also shifted to lower frequencies and their components became less resolved. These spectral changes reflect a strong hydrogen bond system existing in solid state. Since the molecules do not have hydroxyl moieties, it is probable that the cavity of the studied ligands include some water molecules during crystallization, as it was also found before in the case of some calix [4] arenes and cyclodextrins [7,11,12].

Table II shows absorption maxima obtained from the DRIFT spectra of calixarenes **1–5** by curve fitting. Since the N—H and O—H stretching bands are broad, the maxima were estimated from the second derivative spectra. It is interesting to realize that the location of the absorption maxima read directly from the spectra of

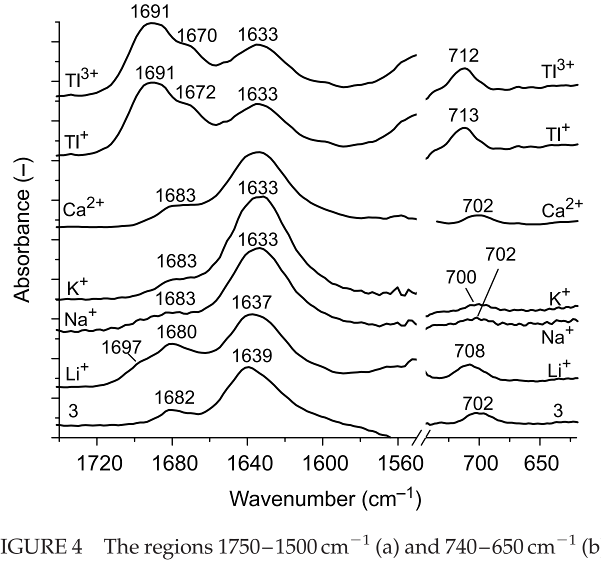

FIGURE 4 The regions 1750–1500 cm^{-1} (a) and 740–650 cm^{-1} (b) of the IR spectra of calixarene **3** in the presence and in the absence of some metal halogenides in acetonitrile solutions. Cations are indicated on the graphs.

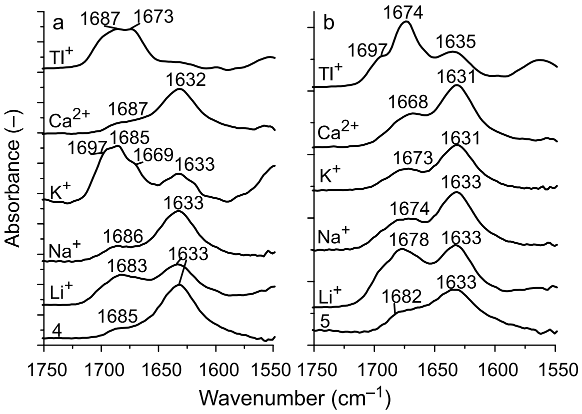

FIGURE 5 The amide-I region of the IR spectra of calixarenes **4** (a) and **5** (b) in the presence and in the absence of some metal halogenides in acetonitrile solutions. Cations are indicated on the graphs.

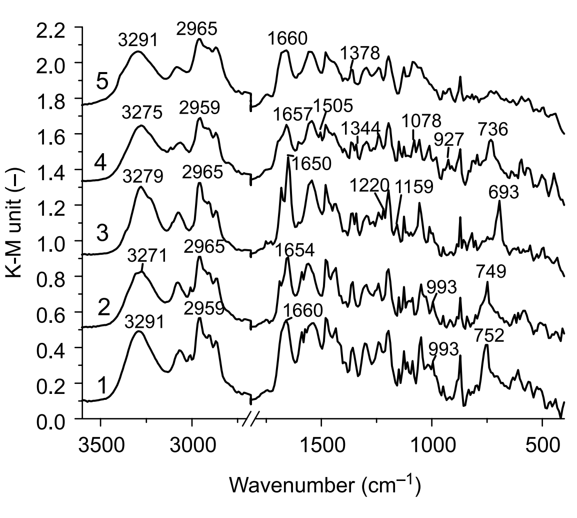

FIGURE 6 DRIFT spectra of calixarenes **1–5** recorded in KBr matrix with pure KBr as reference; spectra of ligands **2–5** are offset for clarity.

chloroform solutions (see Table I) are in good agreement with those obtained by curve fitting. Whereas in case of the DRIFTS results the maxima obtained by peak picking and by curve fitting exhibit somewhat greater deviation from each other. It is likely due to the known fact that hydrogen bond formation causes at ν(OH) stretching mode not only a shift of the involved bands to lower frequencies, increase of the integrated intensity of the band but also considerable broadening as well as, in some cases, mixing of the vibrational modes (see e.g. [22,23]). The locations of O—H stretching modes measured in these DRIFTS experiments are close to those values reported for *p-tert*-butylcalix [4] arene in the partial cone or 1,2-alternate conformation [24]. This fact indicates the weakness of the interaction between the bound water and the ligand. Furthermore, specific vibrations are detected that characterize the heterocycle of the particular calixarenes. Tentative assignments can be presented based on the literature [18,21,24–30]; they are summarized in Table II.

The relative integrated intensity and the location of the group of band components are summarized in Table III. It is clear that, in general, in solid state we can distinguish more band components in the same region than from the solution spectra. Probably, it is due to the effect of crystal field (lattice forces or factor group splitting, see e.g. [25]). It is also remarkable that the amide-I bands are split into two components in the DRIFT spectra and their intensity with respect to the adjoining bands decrease significantly. As can be seen in Fig. 6, the type of the substituting heterocycle influences the resolution of the amide-I bands and the intensity ratio of their components. The changes of the amide-I band probably occur because of different coupling between the carbonyl groups. Since only one component is evident in the liquid spectra, it is probable that the distinct components in the solid spectra originate from the different position of the C═O groups in the unit cell (see e.g. [7]) or the result of coupling of the C═O vibrations of identical positions.

For characterization of the complexation features, surface complexes of ligands **1**–**5** are studied on different alkali/alkaline earth halogenides. Surface complexes are formed while solution of calixarenes are slowly dried onto the surface of solid alkali halogenide salts. Obviously, a mixture of surface complex and neat calixarene can be detected since the calixarene is not transformed into complex form completely in most of the cases. However, these studies also lead to some conclusions (see Figs. 7–11). In these studies, no traces of chloroform were detected. In case of the use of chloroform solution, traces may remain in the complexes that also would cause spectral differences. However, the chloroform traces can be unambiguously identified based on its characteristic absorption bands, e.g. the stretching of the C—H bond at 3010 cm^{-1} (see e.g. [7]). It means that the concentration of the chloroform residue is under the detection limit.

Fig. 7 shows DRIFT spectra of calixarene **1** on sodium chloride, potassium chloride and bromide, and calcium fluoride. The use of a series of potassium salts, i.e. potassium chloride, bromide and iodide ensure the opportunity to observe the effect of the anion of the salt if any. However, these experiments do not serve with relevant additional information in most of the cases because spectra obtained on potassium iodide were too noisy due to the presence of water that cannot be compensated by subtraction (potassium iodide is more hygroscopic than potassium chloride or bromide). It reflects the fact that water interacts with the surface of potassium iodide and this interaction causes the shift of the vibrations of adsorbed water molecules. Thus, only spectra on potassium chloride and bromide and one representative spectrum, the spectrum of calixarene **4**, on the surface of KI are shown in this paper (see Fig. 10). The DRIFTS experiments cannot be carried out on calcium chloride due to the strong hygroscopic character of this salt.

Almost no difference can be seen when comparing the IR spectra of ligand **1** obtained on sodium chloride, potassium chloride and potassium bromide. The only noteworthy, still minor difference in their spectral features is the shift of a skeletal vibrational band that appears at 1562 cm^{-1} on NaCl, at 1561 cm^{-1} on KBr and at 1558 cm^{-1} on KCl. There is a weak band at 669 cm^{-1} in the IR spectrum of ligand **1**-KBr system, that is missing from the other two. Thus, it can be concluded that the calixarene **1** ligand is not selective to any ion in the solid state as detected by DRIFTS.

In the case of calixarene **2**, the experience was surprisingly different (see Fig. 8): major spectral changes are detected while the salt is altered. The spectra—obtained on potassium bromide and chloride—are identical within the error of the measurement. However, several spectral differences are observed in comparison with the DRIFT spectrum recorded on the surface of sodium chloride. A hydroxyl stretching band appears at 3341 cm^{-1} on the potassium salts whereas it is missing from the spectrum of the **2**-NaCl system. Another band at 3288 cm^{-1} shifts to 3269 cm^{-1} while potassium chloride or bromide is substituted by sodium chloride. The maximum of CH stretching mode appears at 2906 cm^{-1} with a shoulder at 2929 cm^{-1} in the spectrum of the sodium complex whereas it is exactly the other way round in the case of the spectra recorded on potassium salts under study. Furthermore, the amide-I vibrational mode appears at 1693 cm^{-1} in the case of potassium salts while the same mode is detected at 1688 cm^{-1} in the

TABLE II Selected vibrations in the DRIFT spectra of calixarenes **1–5** recorded in KBr matrix (sh denotes shoulder, +denots overlapping bands, for explanation of the symbols see [20]).

Assignment and literature	**1**	**2**	**3**	**4**	**5**
	Location (cm^{-1})				
$\nu(NH)^{\dagger}$ and $\nu(OH)^{\dagger}$ [21]	–	3359 sh	3363 sh	–	3396 sh
	3291	3271 + 3311	3279	3275	3291
Amide-I [21]	1747	1747	1749 + 1731	1754 + 1738	1747
	1682 + 1660	1689 + 1654	1682	1696 + 1657	1681 + 1660
			1650		
$\nu(CC)_{rg}$ [18, 21, 29]	–	–	1602	1602	1602
Other vibrational bands	1591 $\nu(CN)_{pyr}$ [30]	1591 $\nu(CN)_{pyr}$ [30]	–	–	–
	1572 $\nu(CN)_{pyr}$ [30]	1568 $\nu(CN)_{pyr}$ [30]	–	–	–
			–	1505 $\nu(CC)_{fur} + \beta(CH)_{fur}$ [27]	–
					1378 sh $\beta(CH)_{thf}$ [27]
	1416 $\delta(CN)_{pyr}$ [30]	1415 $\delta(CN)_{pyr}$ [30]	–	–	–
	–	–	$\sim$1344 $\delta(CH)_{tio} + \nu(CC)_{tio}$ [28]	1344 $\nu(CC)_{fur} + \beta(CH)_{fur}$ [27]	–
			1269 $\delta(CH)_{tio}$ [28]	1263 $\beta(CH)_{fur} + \nu(CO)_{fur} + \nu(CC)_{fur}$ [27]	–
			1220 $\delta(CH)_{tio}$ [28]	–	–
			1159 $\nu(CC)_{tio}$ [25] (based on 2,2′-bithiophene)	–	–
			–	1078 $\nu(CO)_{fur} + \nu(CC)_{fur} + \beta(CH)_{fur}$ [27]	–
	993	993	–	–	–
			–	927 $\gamma(CH)_{fur}$ [27]	–
			854 $\nu(CS)_{tio} + \delta(CC)_{tio}$ [25,28]	–	–
	752	749	–	736 $\gamma(CH)_{fur}$ [27]	–
			693 $\gamma(CH)_{tio}$ [25,28]	–	–

†These values are read from the second order derivative of the spectra.

TABLE III Relative integrated intensity of the IR band components of calixarenes **1**–**5** in the hydroxyl and amide-I regions detected in chloroform solution and in solid state as revealed by curve fitting (for explanation of the symbols see [20]).

Calixarene	Chloroform solution			DRIFTS		
	Assignment	Location	Relative. Intensity	Assignment	Location	Relative. Intensity
1	ν(NH)	3436	0.15	ν(NH) and ν(OH)	3380	0.03
	ν(OH)	3341	0.80		3296	0.83
		3225	0.05		3187	0.14
	Amide-I	–	–	Amide-I[†]	1770	0.05
		1751	0.02		1746	0.02
		1679	0.34		1686	0.25
		1663	0.64		1658	0.68
2	ν(NH)	3432	0.09	ν(NH) and ν(OH)	3360	0.01
	ν(OH)	3337	0.63		3293	0.67
		3226	0.28		3216	0.31
	Amide-I	–	–	Amide-I[†]	1784	0.08
		1765	0.01		1747	0.03
		1674	0.45		1690	0.18
		1658	0.54		1654	0.71
3	ν(NH)	3432	0.05	ν(NH) and ν(OH)	3367	0.02
	ν(OH)	3334	0.91		3288	0.61
		3211	0.04		3215	0.37
	Amide-I	–	–	Amide-I[†]	1777	0.04
		1751	0.02		1749	0.02
		–	–		1731	0.05
		1679	0.34		1682	0.37
		1663	0.64		1649	0.52
4	ν(NH)	3434	0.21	ν(NH) and ν(OH)	3375	0.05
	ν(OH)	3339	0.60		3297	0.39
		3225	0.19		3229	0.56
	Amide-I	–	–	Amide-I[†]	1792	0.03
		1765	0.01		1755	0.06
		–	–		1696	0.43
		1676	0.44		1680	0.01
		1662	0.55		1657	0.46
5	ν(NH)	3436	0.10	ν(NH) and ν(OH)	3388	0.09
	ν(OH)	3345	0.73		3319	0.62
		3280	0.16		3234	0.29
	Amide-I	–	–	Amide-I[†]	1775	0.05
		1751	0.01		1750	0.06
		–	–		1735	0.01
		1666	0.97		1687	0.43
		1659	0.02		1657	0.45

[†] Since four amide groups are present in each ligand, there should be maximum four band components in amide-I band. Probably C—O modes are superimposed with the amide-I bands.

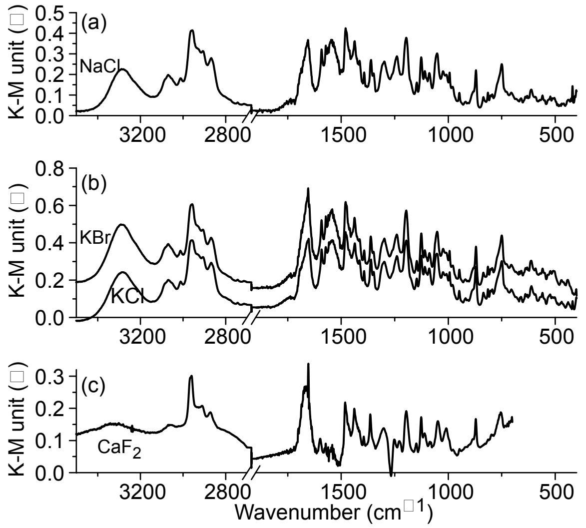

FIGURE 7 DRIFT spectra of the surface complexes of calixarene **1** formed on (a) sodium chloride; (b) potassium chloride and bromide; and (c) calcium fluoride. Salts are indicated on the graphs.

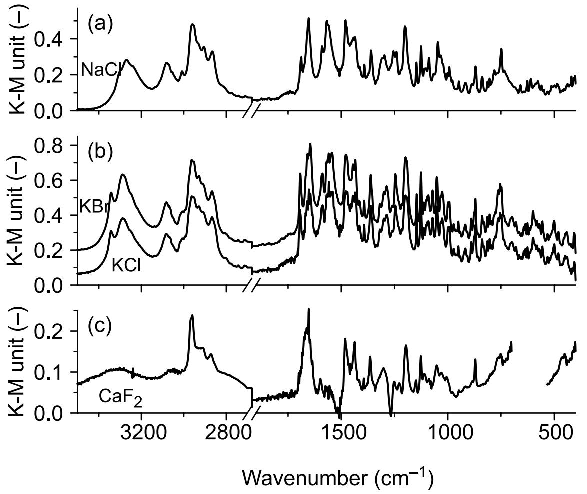

FIGURE 8 DRIFT spectra of the surface complexes of calixarene **2** formed on (a) sodium chloride; (b) potassium chloride and bromide; and (c) calcium fluoride. Salts are indicated on the graphs.

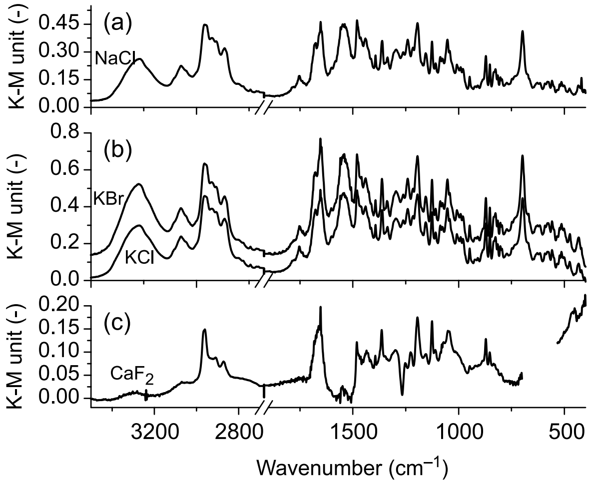

FIGURE 9 DRIFT spectra of the surface complexes of calixarene **3** formed on (a) sodium chloride; (b) potassium chloride and bromide; and (c) calcium fluoride. Salts are indicated on the graphs.

case of sodium chloride support. An overlapping band of skeletal vibrational modes gives rise to a maximum at 1654 cm^{-1} on NaCl, whereas in the spectra recorded on potassium salts three maxima at 1659, 1653 and 1646 cm^{-1} are observed with the highest intensity at 1646 cm^{-1}. With the $\nu(\mathrm{CN})_{\mathrm{pyr}}$ band at 1590 cm^{-1} another component overlaps centered at 1588 cm^{-1} in the spectra of **2**-potassium salt systems. Deformational vibrational modes are more intense in the spectrum of sodium complex at 1568, 1480 and 1201 cm^{-1}, while those observed at 1558, 1445, 1435 and 1192 cm^{-1} are noticeably more intense in the spectra detected on potassium supports. Absorption maxima appear at 1287 and 1072 cm^{-1} recorded on potassium chloride and bromide that are lacking in the spectrum of the sodium complex.

The above list of the major spectral changes is not exhaustive, however all these changes support the existence of a sodium/potassium selectivity. These facts also mean that the addition of a methylene unit in the "arms" of the complexation sphere increase the selectivity of the derivatives carrying pyridine moieties.

The comparison of the DRIFT spectra of ligand **3** obtained on sodium chloride, potassium chloride and potassium bromide (Fig. 9), results in almost as few conclusions as in the case of ligand **1**. The characteristic $\gamma(\mathrm{CH})_{\mathrm{tio}}$ appears at 698 cm^{-1} and it is rather insensitive to the nature of the alkali/alkaline earth ion used in this study. The spectrum recorded on the surface of potassium iodine is rather noisy (not shown in this paper) due to the presence of moisture; however, the signal-to-noise ratio is efficient for realizing that the spectrum is somewhat different from those obtained on potassium chloride or bromide and sodium chloride. The most significant difference is exhibited in the stretching mode of CH moieties, i.e. the intensity of the absorption band is higher at 2906 cm^{-1} than at 2923 cm^{-1} in the case of potassium iodine, whereas that of 2927 and 2906 cm^{-1} is in the opposite order in the case of other potassium salts and sodium chloride, and the 2923 cm^{-1} band also shifts to higher frequencies. That band at 2927 cm^{-1}is broader than its counterpart in the spectrum on KI and more band components are discernible under the envelope.

Calixarene **4** also exhibits surprising complexation characteristics, as illustrated in Fig. 10. Differences between the DRIFT spectra obtained on sodium chloride, potassium chloride and bromide can be hardly noticed. However, the spectrum recorded on potassium iodine is remarkably different from the aforementioned ones. The OH stretching bands are rather broad, the componenrs are obtained by resolution. Two additional OH stretching band components are detected at 3355 and 3436 cm^{-1}, these are probably characteristic of water-iodine ion interactions on the surface of the salt. The presence of these bands support the conclusion that water vapour interacts with the solid sample. In the high frequency region, the most significant difference is exhibited in the stretching mode of CH moieties, similarly to ligand **3**. The intensity of the adsorption band is higher at 2904 cm^{-1} than at 2922 cm^{-1} in the case of potassium iodine, whereas that of 2928 and 2907 cm^{-1} is in the opposite order in the case of other potassium salts and sodium chloride as revealed by curve-fitting. The bands also shift somewhat as it can be seen from the values of their locations. An intense band at 1659 cm^{-1} is missing from the spectrum obtained on KI support, however it is present in the other spectra. Similarly, the overlapping bands at 1543 and 1585 cm^{-1} are not present in the IR

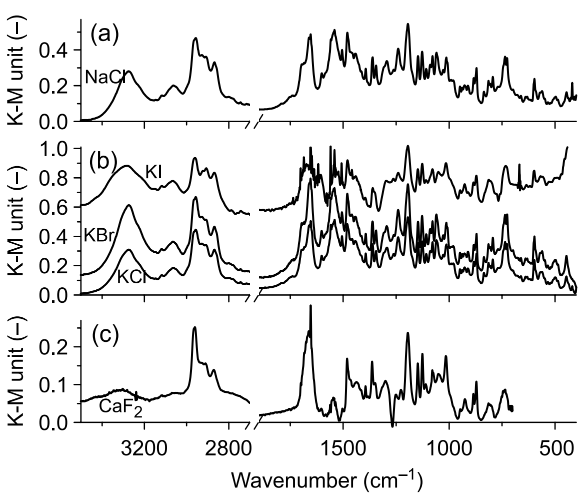

FIGURE 10 DRIFT spectra of the surface complexes of calixarene **4** formed on (a) sodium chloride; (b) potassium chloride, bromide and iodide; and (c) calcium fluoride. Salts are indicated on the graphs.

spectrum measured on KI. It is possible that the missing bands are broadened and merged under the envelope because of the presence of hygroscopic water of higher quantity. In the spectra of ligand **4** on sodium chloride, potassium chloride and bromide, two absorption bands show up at 1362 and 1345 cm^{-1} a "two-humped" shaped envelope, whereas in the spectrum of the **4**-KI system, a shoulder is evident at 1351 cm^{-1} on the absorption maximum at 1362 cm^{-1}. The skeletal and/or deformational bands or band components at 1309, 1090 and 1028 cm^{-1} are lacking on potassium iodine. The vibrational band at 1060 cm^{-1} has a shoulder at 1052 cm^{-1}, while in the spectrum obtained on KI only one band can be seen at 1052 cm^{-1}, the 1060 cm^{-1} component diminishes. The intensity of the absorption maxima at 1295 and 1242 cm^{-1}, significantly reduces when the potassium iodine is used instead of other potassium salts or sodium chloride. The list of detected spectral changes is far from complete, but one can assume that in case of potassium iodine ligand **4** interacts with the K^+I^- ion pair whereas the chloride or bromide does not participate in the interaction or they participate in a different manner.

Calixarene **5** exhibits very different complexation properties in solid state (see Fig. 11). Certainly, the detected spectra do not differ drastically from each other. However, the most notable changes are the following. In the region of higher frequencies a hydroxyl stretching band component appears at 3086 cm^{-1} on potassium bromide. The same component overlaps with another one at 3065 (on NaCl) and at 3073 cm^{-1} (KCl) and these components are the maxima of the overlapping group of bands. Envelopes are identical in the other part of this region. The envelope of amide-I vibrational mode also consists of some components from which the one at 1684 cm^{-1} is missing from the DRIFT spectrum of **5**-KBr system. The skeletal band shifts from 1551 cm^{-1} (on KBr) to 1548 cm^{-1} (on KCl) and 1542 cm^{-1} (on NaCl). From these changes it seems that calixarene **5** also exhibits anion selectivity over alkali ions. These indicative properties towards anions are in accordance with earlier observations obtained by NMR spectroscopy [32].

As it can be seen in Figs. 7–11, the spectra on calcium fluoride are rather distorted in the regions of 3940–3010, 1615–1500 and 1300–1230 cm^{-1}. As known from the literature [34], calcium fluoride windows exhibit excellent transmission from 150 nm to 7 μm, i.e. between 667000 and 1428 cm^{-1} and a sharp cutoff at 12 μm (under 833 cm^{-1}, 1.19 mm sample thickness). However, calcium fluoride readily adsorbs water molecules on its surface (see e.g. [34]) and independent experiments revealed that the infrared spectrum of calcium fluoride has broad absorption maxima centered at around 3410 and 1630 cm^{-1} (the deformation of R—OH is detected at much lower frequencies). Thus, the distortion of the DRIFT spectra of calixarenes **1–5** indicates the presence of significant amount of adsorbed water on the surface of calcium fluoride.

FT–Raman Measurements

As it was mentioned above, Raman spectra of the surface complex samples were also detected. In the literature examples are found (see e.g. [13]) when even the conformation of the ligand could be estimated in complex form based on their Raman spectra. Raman spectra of the untreated salts, i.e. the backgrounds of the Raman experiments are also recorded and shown in Fig. 12. As it can be seen,

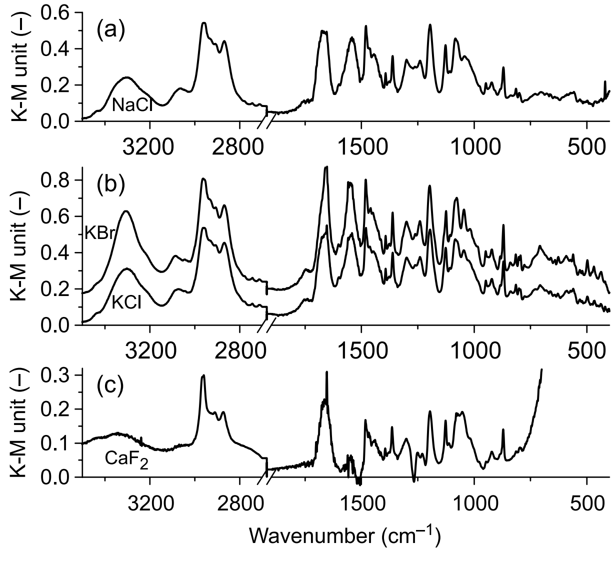

FIGURE 11 DRIFT spectra of the surface complexes of calixarene **5** formed on (a) sodium chloride; (b) potassium chloride and bromide; and (c) calcium fluoride. Salts are indicated on the graphs.

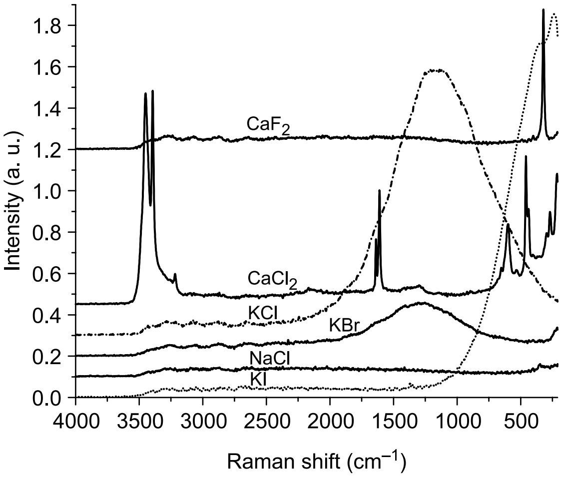

FIGURE 12 FT–Raman spectra of the pure alkali/alkaline earth halogenide salts under study, i.e. backgrounds of the Raman measurements; salts are indicated on the graphs, spectra of sodium chloride, potassium chloride, potassium bromide, calcium fluoride and calcium chloride are offset for clarity.

potassium chloride and iodide exhibit very intense Raman scattering over a wide region that cause noisy spectrum and thus, the loss of information about the Raman signal of the ligands. It can also be seen that the Raman spectrum of calcium chloride is rather rich in lines that is also due to strong hygroscopic character of this salt (we did not manage to dry the samples completely). Raman spectra obtained with calcium chloride as solid support and substrate will be discussed later in this chapter. A minor interference is superimposed with the recorded Raman spectra that are characteristic of the optical system used. However, this phenomenon can be easily eliminated by subtraction. The Raman spectra on potassium iodide were not analyzed, either, since—as it is mentioned above—they did not yield relevant conclusions.

In general, Raman spectra obtained in this study are found not sensitive enough to complex formation (see Fig. 13 for illustration). Furthermore, it is not possible to differentiate between complexes of the same ligand formed on different salt surfaces, probably, because of the relatively poor signal-to-noise ratio of the spectra. As it is known Raman lines appear in the case of those vibrational modes during which polarizability of the molecule changes [35]. It seems that complex formation of calixarenes **1**–**5** in solid sate does not result in detectable changes of the polarizability in the involved chemical bonds under the measurement conditions used. Therefore only one set of representative spectra (one for each studied calixarene) is shown in Fig. 14. Tentative assignment of the major Raman lines are also presented (see also Table IV).

As it was mentioned above, the Raman spectrum of calcium chloride is quite rich in lines (see Fig. 15) and the presence of relatively many Raman peaks is also the consequence of the strong hygroscopic

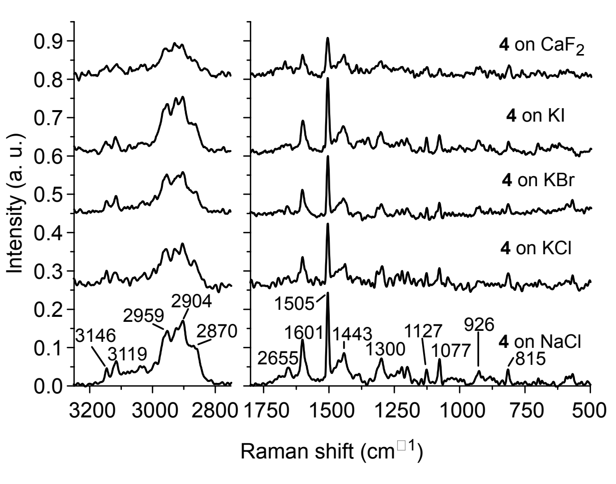

FIGURE 13 FT–Raman spectra of the surface complexes of calixarene **4** formed on different metal halogenides. (a) sodium chloride; (b) potassium chloride; (c) potassium bromide; (d) potassium iodide; and (e) calcium fluoride. Salts are indicated on the graphs.

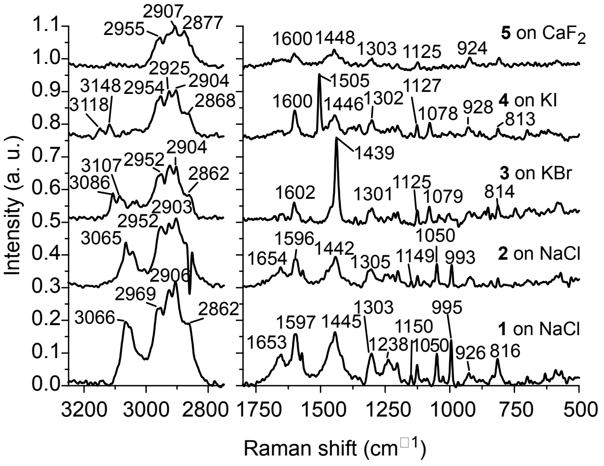

FIGURE 14 Some Raman spectra of the surface complexes of calixarene **1**–**5** formed on different salts (a) Calixarene **1**—sodium chloride; (b) Calixarene **2**—sodium chloride; (c) Calixarene **3**—potassium bromide; (d) Calixarene **4**—potassium iodide; and (e) Calixarene—calcium fluoride, as indicated on the graph.

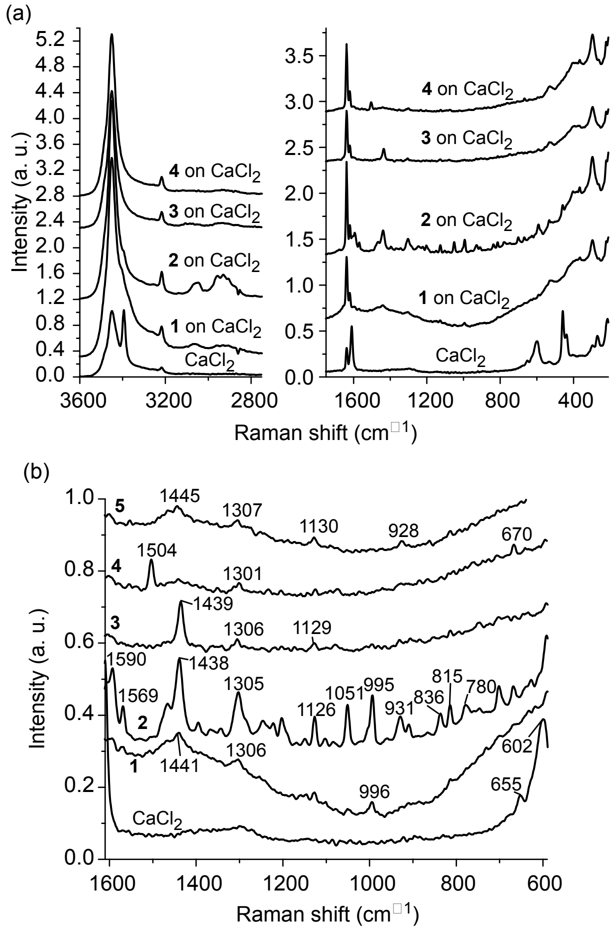

FIGURE 15 Raman spectra of the surface complexes formed by calixarenes **1**–**5** on calcium chloride and the reference spectrum of untreated calcium chloride in the regions of (a) 3600–2750 and 1750–210 cm^{-1}; (b) zoomed between 1620 and 600 cm^{-1}. Ligands are indicated on the graphs; spectra of the ligands are offset for clarity.

TABLE IV Selected vibrations in the Raman spectra of solid calixarenes **1**–**5** (sh denotes shoulder, the assignments are based on the literature written below, for explanation of the symbols see [20]).

Assignment and Literature	**1**	**2**	**3**	**4**	**5**
	Location (cm^{-1})				
$\nu(OH) + \nu(NH)$ [21, 36]	3280 br	3277 br	3263 br	3277 br	3307 br
	3180 br $\nu(OH\ldots N_{pyr})$	3178 br $\nu(OH\ldots N_{pyr})$		3146 $\nu(OH\ldots O_{fur})$	
$\nu(CH)_{ar}$ of heteroaromatic ring and skeleton $+\nu(CH_3) + \nu(CH_2)$ [18, 21, 29]	3137	3137	3108	3125	
	3070	3070	3087	3118	
				3113	
	3049	3045	3073	3077	3073 sh
	3011	3009	3051	3033	3024
$\nu(CH_2)$ and $\nu(CH_2)$ of skeleton [21]	2967 sh	2966 sh	2969 sh	2997 sh	2965 sh
	2952	2951	2950	2956	2953
	2928	2927	2927	2926	2927
	2903	2903	2903	2903	2903
	2777	2776	2778	2779	2779
	2709	2707	2709	2706	2709
Amide-I [21]			1683	1691 sh	1680 sh
	1677 sh	1674	1673	1658	1657
	1652	1655	1653	1646 sh	
$\nu(CC)_{rg}$ [21]	1600	1601	1599	1600	1599
	1591 $\nu(CN)_{pyr}$ [30]	1590 $\nu(CN)_{pyr}$ [30]	1582 $\nu(CC)_{rg}$ [21]	1580 sh $\nu(CC)_{rg}$ [21]	1583 sh $\nu(CC)_{rg}$ [21]
Other vibrational bands	1570 $\nu(CC)_{pyr} + \beta(CC)_{pyr}$ [30]	1569 $\nu(CC)_{pyr} + \beta(CC)_{pyr}$ [30]			
			1538 $\nu(CC)_{tio} + \delta(CH)_{tio}$ [28]		
				1504 $\nu(CC)_{fur} + \beta(CH)_{fur}$ [27]	
				1385 $\nu(CC)_{fur} + \beta(CH)_{fur}$ [27]	
				1298 $\beta(CH)_{fur}$ [27]	
			1080 $\delta(CH)_{tio} + \nu(CC)_{tio}$ [28]	1078 $\nu(CC)_{fur}$ [27]	
	1050 $\nu(CC)_{pyr} + \delta(CH)_{pyr}$ [30]	1051 $\nu(CC)_{pyr} + \delta(CH)_{pyr}$ [30]			
	994	994			
					922 $\beta(CH)_{thf} + \nu(CC)_{thf} + \nu(CO)_{thf}$ [27]
				884 $\beta(CC)_{fur}$ [27]	882 $\nu(CC)_{thf} + \beta(CH)_{thf}$ [27]
			866 $\gamma(CH)_{tio}$ [28]		
			853 $\nu(CS)_{tio} + \delta(CC)_{tio}$ [25,28]	857 $\gamma(CH)_{fur}$ [27]	
	835	840			
	773 $\beta(CC)_{pyr} + \nu(CC)_{pyr} + \delta(CH)_{pyr} + \nu(CN)_{pyr}$ [30]	780 $\beta(CC)_{pyr} + \nu(CC)_{pyr} + \delta(CH)_{pyr} + \nu(CN)_{pyr}$ [30]			
			749 744 sh $\beta(CH)_{tio}$ [25]		
			666 $\gamma(CH)_{tio}$ intermolecular forces [25,28]		
				647	
				641	
	590 $\beta(CC)_{pyr} + \delta(CN)_{pyr}$ [30]	582 $\beta(CC)_{pyr} + \delta(CN)_{pyr}$ [30]	583 $\beta(CC)_{tio}$ [31]		587
	568 $\beta(CC)_{pyr} + \nu(CC)_{pyr}$ [30]	570 $\beta(CC)_{pyr} + \nu(CC)_{pyr}$ [30]		568	
			476 $\tau(CH)_{tio}$ [31]		

character of this salt. It is interesting that in the 3600–3000 cm^{-1} region the envelope of the spectrum is analogous to the Raman spectrum of frozen aqueous calcium chloride solution but, certainly, the bands are shifted [36]. However, the attachment of ligands **1–5** caused significant spectroscopic changes. Therefore it is worth to draw a few conclusions from these spectra (see Fig. 15 and Table IV). The NH stretching mode of acid amides in Raman spectra is usually broad and quite weak (see, e.g. in [31]) and they overlap with the stretching bands of bound water in the region of 3400–3150 cm^{-1}. Therefore it is not possible to assign any separate peak of the studied ligands to ν(NH). The bands at higher frequencies correspond to ν(OH) bands where the hydroxyl groups are bound in different extent and various manners. The component at 3395 cm^{-1} is detected in the case of the untreated calcium chloride and it disappears from the spectra of the studied ligand—$CaCl_2$ systems. It is characteristic for one of the band components of pure water or 1 M aqueous calcium chloride solution and is assigned as completely hydrogen bonded water molecules [37]. The other two intense components of pure water or 1 M aqueous calcium chloride solution centered at 3233 cm^{-1} (four fully hydrogen bonded water structures) and 3511 cm^{-1} (their hydrogen bonds have been broken in part or totally) are not detected. As expected, these facts indicate that the amount of water did not reach that quantity that is enough for the formation of water–water hydrogen bonds, and water molecules cannot be free on the surface of an alkali earth halogenide due to water–salt coulombic interactions (see also data in Table V).

The intensity of deformation mode of water at around 1639 cm^{-1} increases about double of that in the pure calcium chloride hydrate, whereas the preak centered at ~1610 cm^{-1} diminishes when any of calixarenes **1–5** is adsorbed on its surface. However, the band located at 1621 cm^{-1} that appears as a shoulder in the Raman spectrum of the pure calcium chloride hydrate, is characterized with almost constant intensity in every Raman spectrum recorded on the same salt support. These bands can be assigned to the bending vibration of water and in line with the high-frequency-bands, the relatively sharp line at 1610 cm^{-1} corresponds to bonded water molecules at a specific location of the salt grind. From the analysis of these spectral changes, it is obvious that the interaction between calixarenes **1–5** and calcium chloride is connected with changes in the attachment of water of crystallization. It is reasonable to assume that the interaction between the ligand and the salt occurs at the active sites by squeezing out water molecules from special locations of the crystal surface.

TABLE V The water content of the neat, solid ligands **1–5** were determnined by a Mettler Toledo Coulometric Karl-Fischer titrator (Coulometer DL 39) in Hydranal®–Coulomat AG reagent (produced by Riedel-de Haën). The water contents are the following.

Ligand	Water content (mass %)	X, molar ratio of water (calixarene:water=1:X)
1	1.74	~1.20
2	0.89	~0.60
3	0.39	~0.25
4	0.33	~0.20
5	1.21	~0.80

The studied calixarenes were not dried before the experiments since for the DRIFTS experiments the solid compounds are dissolved preparation and the complexes are dried later during the sample. The hygroscopic character of the alkali/alkali earth halogenides are much more significant from the pont of view of final moisture content of the complexes than the water content of the organic starting componds, thus the effect of the letter ones are likely negligible.

Between 1600 and 600 cm^{-1}, various Raman bands are recorded that correspond to calixarenes **1–5**. As apparent in Fig. 15b, the best signal-to-noise ratio is achieved in the case of the ligand **2**—$CaCl_2$ system. The spectrum of **3** is somewhat and that of **4** is rather noisy, therefore the locations of Raman lines are less certain than in the case of the other Raman spectra. The assignment of the characteristic Raman lines are also tabulated in Table VI.

In the fingerprint region under 600 cm^{-1}, the Raman spectra of the studied calixarenes exhibit a similar envelope on the surface of calcium chloride. Raman lines of the studied ligands and water of crystallization are superimposed with each other. Some bands appear in all of these spectra, e.g. the band at 299 cm^{-1} (weak) does not shift significantly (to 300 or 297 cm^{-1}), however, it becomes a strong band when calixarenes **1–5** are attached on the surface of calcium chloride. The line at 270 cm^{-1} also shifts somewhat to the lower frequencies. The assignment of the bands under 400 cm^{-1} cannot be found in the cited literature [25,27,28,30]. However, the assignment in the fringerprint region in general is a so difficult task due to the complex nature of these vibrational modes that would probably not lead to significant and unambiguous conclusions.

In the column of $CaCl_2$ hexahydrate in Table V, many bands are shown without assignment. Those bands were not detected by Winnett and Nash [38]. It is probable that the composition of our hydrous salt was not exactly stoichiometric due to the preliminary drying of the samples, the heating–drying effect of the Nd:YAG laser used for excitation in the Raman spectrometer, and the strongly hygroscopic character of the salt. Thus those vibrational modes are also detected that are characteristic of other cluster structers. It is in line with the remark in Ref. [38], which says that the calcium chloride hexahydrate crystals have quite inferior optical quality in

TABLE VI Selected vibrations in the Raman spectra of solid calixarenes **1**–**5** on the surface of calcium chloride (sh denotes shoulder, deformations: w = wagg, r = rock; the assignments are based on the literature written below, for explanation of the symbols see [20]).

Assignment and literature	**1**	**2**	**3**	**4**	**5**	$CaCl_2$
	Location (cm^{-1})					
ν(OH) water + ν(NH) [21,36,37] (overlapping)	3451	3451	3451	3451	3457	3451
	3400 sh	3394 sh				3395*
	3369 sh					
ν(OH) water [37]	3218	3217	3217	3217	3222	3217
			3110 $\nu(\mathrm{CH})_{\mathrm{tio}}$ [28]			
$\nu(\mathrm{CH})_{\mathrm{ar}}$ [21]	~3060 k $\nu(\mathrm{CH})_{\mathrm{pyr}}$ [30]	3066	~3081 k + $\nu(\mathrm{CH})_{\mathrm{tio}}$ [28]	Noisy		–
		3060				
		3045 $\nu(\mathrm{CH})_{\mathrm{pyr}}$ [30]				
$\nu(\mathrm{CH}_2)$ [20]	2965	2957			2969	–
	2930	2930	~2937 k	~2926 k	2930	
	2906	2905			2905	
	2869 sh	2867 sh	2871 sh		2869 sh	
Water [37] + Amide-I [21]	1638	1638	1638	1639	1638	1639 δ(OH)
	1620	1620	1620	1618	1620	1618
	–	–	–	–		1610* δ(OH)
	1590 $\nu(\mathrm{CC})_{\mathrm{pyr}}+\nu(\mathrm{CN})_{\mathrm{pyr}}$ [30]	1592 $\nu(\mathrm{CC})_{\mathrm{pyr}}+\nu(\mathrm{CN})_{\mathrm{pyr}}$ [30]				
Other vibrational bands	~1568 $\nu(\mathrm{CC})_{\mathrm{pyr}}+\beta(\mathrm{CC})_{\mathrm{pyr}}$ [30]	1569 $\nu(\mathrm{CC})_{\mathrm{pyr}}+\beta(\mathrm{CC})_{\mathrm{pyr}}$ [30]				
	–	–		1504 $\nu(\mathrm{CC})_{\mathrm{fur}}+\beta(\mathrm{CH})_{\mathrm{fur}}$ [27]		
	~1468 sh $\beta(\mathrm{CH})_{\mathrm{pyr}}+\nu(\mathrm{CC})_{\mathrm{pyr}}+\nu(\mathrm{CN})_{\mathrm{pyr}}$	1467 sh $\beta(\mathrm{CH})_{\mathrm{pyr}}+\nu(\mathrm{CC})_{\mathrm{pyr}}+\nu(\mathrm{CN})_{\mathrm{pyr}}$			1466sh	
	1441 $\beta(\mathrm{CH})_{\mathrm{pyr}}$ [30]	1439 $\beta(\mathrm{CH})_{\mathrm{pyr}}$ [30]				
					1445 $\gamma(\mathrm{CH})_{\mathrm{thf}}$ [27]	
			1435 $\nu(\mathrm{CC})_{\mathrm{tio}}+\beta(\mathrm{CH})_{\mathrm{tio}}$ [28]			
	1439 $\beta(\mathrm{CH})_{\mathrm{pyr}}$ [30]	1439 $\beta(\mathrm{CH})_{\mathrm{pyr}}$ [30]				
		931 $\gamma(\mathrm{CH})_{\mathrm{pyr}}$ [30]				
		910 $\gamma(\mathrm{CH})_{\mathrm{pyr}}$ [30]				
		836				
		813 $\beta(\mathrm{CC})_{\mathrm{pyr}}+\nu(\mathrm{CC})_{\mathrm{pyr}}$ [30]				
		702 $\delta(\mathrm{CN})_{\mathrm{pyr}}+\gamma(\mathrm{CH})_{\mathrm{pyr}}$ [30]				
		670 $\delta(\mathrm{CN})_{\mathrm{pyr}}+\gamma(\mathrm{CH})_{\mathrm{pyr}}$ [30]				
						602 r [37]
		592 $\beta(\mathrm{CC})_{\mathrm{pyr}}+\delta(\mathrm{CH})_{\mathrm{pyr}}$ [30]				
		533 $\delta(\mathrm{CH})_{\mathrm{pyr}}+\beta(\mathrm{CC})_{\mathrm{pyr}}$ [30]				
		461 $\delta(\mathrm{CC})_{\mathrm{pyr}}+\gamma(\mathrm{CC})_{\mathrm{pyr}}+\delta(\mathrm{CN})_{\mathrm{pyr}}$ [30]				461 w [37] 436
	403 br $\delta(\mathrm{CC})_{\mathrm{pyr}}+\delta(\mathrm{CN})_{\mathrm{pyr}}+\gamma(\mathrm{CH})_{\mathrm{pyr}}$	403 $\delta(\mathrm{CC})_{\mathrm{pyr}}+\delta(\mathrm{CN})_{\mathrm{pyr}}+\gamma(\mathrm{CH})_{\mathrm{pyr}}$	398 br	400 br		
	365 $\delta(\mathrm{CH})_{\mathrm{pyr}}$ [30]	367 $\delta(\mathrm{CH})_{\mathrm{pyr}}$ [30]	365	366		
$\tau(\mathrm{CaCl_2}\ldots\mathrm{H_2O})$ [31, 37]	300	297	297	297		299
$\tau(\mathrm{CaCl_2}\ldots\mathrm{H_2O})$ [31, 37]	260 sh	262 sh	259 sh	264 sh		270

comparison with the stroncium counterparts therefore the spectroscopic measurements had to be repeated many times to ensure the validity of the results.

SUMMARY

In the present paper, five tetraamido-type calix[4]-arene derivatives are examined by vibrational spectroscopic techniques. First, the transmission FT–IR spectra of acetonitrile solutions of these ligands are recorded in the presence of various metal halogenides. In agreement with our earlier experience [6,7,21], differentiation is found between the cations on the basis of infrared spectra (with special emphasis on the amide-I vibrational mode) in these solution experiments. The most advantageous was the application of thiophene derivative **3**, which exhibits selective complex formation with thallium ions as detected at a characteristic amide-I band of the thallium complex at 1691 cm^{-1} and also at the $\gamma(\mathrm{CH})_{\mathrm{tio}}$ absorption band at around 700 cm^{-1}. This latter result supports the conclusion that the heteroatom of the heteroaromatic ring participates in the complex formation. Calixarenes **2** and **4** exhibit selectivity to potassium ions and ligand **5** is selective to lithium ions among alkali/alkaline earth ion sin acetonitrile. However, thallium(I) ion tends to form complexes of similar spectral characteristics, thus disturbs the measurements.

In the solid state, calixarenes **1–5** are observed as surface complexes. DRIFTS measurements revealed that calixarene **1** and **5** do not exhibit sufficient selectivity for analitical purposes. The solid state experiments also show that the ligands **3** and **4** are sensitive to the anion as well as to the cation, in line with preliminary results. Calixarenes **2** and **4** are of potential analytical application for the recognition of cations among alkali/alkaline earth metal ions in solid state if FT–IR spectroscopy is used for detection. It is also clear that the number of methylene units in the ”arms” of calixarenes influence the outcome of the complexation process significantly, as it can be seen from the comparison of ligands **1** and **2**.

FT–Raman spectrioscopy is not ideal to detect the differences between different surface complexes formed. However, it detects special features that are characteristic of the ligand-calcium chloride systems. It is evident that the attachment of the ligand molecules on the salt surface is accompanied by the squeezing out the water molecules from some special positions of the hydrated salt grind. The choice of anion does not seem to influence the Raman spectrum.

Acknowledgements

The authors are grateful to Prof. Ferenc Billes (Department of Physical Chemistry, Budapest University of Technology and Economics) for his helpful suggestions and to Prof. Gábor Keresztury (Institute for Structural Chemistry, Chemical Research Center of the Hungarian Academy of Sciences) for his technical assistance and linguistic corrections.

References

[1] Vicens, J.; Böhmer, V. *Calixarenes—A Versatile Class of Macrocyclic Compounds*; Kluwer Academic Publishers: Dordrecht, 1991.
[2] Brzezinski, B.; Bartl, F.; Zundel, G. *J. Phys. Chem. B* **1997**, *101*, 5611.
[3] Mohammed-Ziegler, I.; Kubinyi, M.; Grofcsik, A.; Grün, A.; Bitter, I. *J. Mol. Struct.* **1999**, *480/481*, 289.
[4] Lynam, C.; Jennings, K.; Nolan, K.; Kane, P.; McKervey, M. A.; Diamond, D. *Anal. Chem.* **2002**, *74*, 59.
[5] Hamdi, A.; Abidi, R.; Ayadi, M. T.; Thuéry, P.; Nierlich, M.; Asfari, Z.; Vicens, J. *Tetrahedron Lett.* **2001**, *42*, 3595.
[6] Mohammed-Ziegler, I. *Spectrochim. Acta. A.* **2003**, *59*(1), 19.
[7] Mohammed-Ziegler, I. *Spectrochim. Acta. A.* **2003**, *59*(14), 3239.
[8] Brzezinski, B.; Urjasz, H.; Zundel, G. *J. Phys. Chem.* **1996**, *100*, 9021.
[9] Kunsági-Máté, S.; Nagy, G.; Kollár, L. *Anal. Chim. Acta.* **2001**, *428*(2), 301.
[10] Kunsági-Máté, S.; Szabó, K.; Lemli, B.; Bitter, I.; Nagy, G.; Kollár, L. *Thermochimica Acta.* **2005**, *425*(1–2), 121.
[11] Egyed, O. *Vibr. Spectrosc.* **1990**, *1*(2), 225.
[12] Egyed, O.; Weiszfeiler, V. *Vibr. Spectrosc.* **1994**, *7*(1), 73.
[13] Egyed, O.; Izvekov, V. P. *Spectrosc. Lett.* **1989**, 22(4), 387.
[14] Egyed, O.; Izvekov, V. P.; Tóth, K.; Holly, S.; Pungor, E. *J. Mol. Struct.* **1990**, *218*, 135.
[15] Ivanova, I. S.; Dorokhov, A. V.; Pyatova, E. N.; Galkina, E. N.; Yakshin, V. V.; Tsivadze, A. Yu. *Russ. J. Coord. Chem.* **2005**, *31*(3), 151.
[16] Nissink, J. W. M.; Boerringer, H.; Verboom, W.; Reinhoudt, D. N.; van der Maas, J. H. *J. Chem. Soc. Perk. Trans. 2* **1998**(12), 2623.
[17] Lutz, B. T. G.; Astarloa, G.; Van der Maas, J. H.; Janssen, R. G.; Verboom, W.; Reinhoudt, D. N. *Vibr. Spectrosc.* **1995**, *10*(1), 29.
[18] Billes, F.; Mohammed-Ziegler, I. *Supramol. Chem.* **2002**, *14*(5), 451.
[19] Hamdi, A.; Abidi, R.; Asfari, Z.; Vicens, J. *J. Inclu. Phen. Macrocyclic Chem.* **2003**, *45*, 99.
[20] The following symbols are used in this paper: as usual in the practice of vibrational spectroscopy, the symbol ν denotes stretching vibration, δ in-plane bending and γ out-of-plane bending. β denotes a bending vibration without describing the direction with respect to the plane defined by the atoms, and τ is the symbol for a torsional vibration. Furthermore, rg denotes vibrations corresponding to ring atoms in the calixarene skeleton, pyr deontes the pyridenyl ring, fur symbolizes the furanyl ring, tio is the subscript for thiofenyl ring and thf denotes the tetrahydrofuranyl ring. Sh abbreviates shoulder and br means broad band
[21] Mohammed-Ziegler, I.; Grün, A. *Spectrochim. Acta. A.* **2005**, *62*(1–3), 506.
[22] Kovács, A.; Izvekov, V.; Zauer, K.; Ohta, K. *J. Phys. Chem. A* **2001**, *105*, 5000.
[23] Mohammed-Ziegler, I.; Billes, F. *J. Mol. Struct.-THEOCHEM* **2002**, *618*, 259.
[24] Furer, V. L.; Borisoglebskaya, E. I.; Kovalenko, V. I. *Spectrochim. Acta. A.* **2005**, *61*(1–2), 355.
[25] Zerbi, G.; Chierichetti, B.; Ingänas, O. *J. Chem. Phys.* **1991**, *94*(6), 4637.
[26] Bánki, J.; Billes, F.; Gál, M.; Grofcsik, A.; Jalsovszky, G.; Sztraka, L. *Acta. Chim. Hung.* **1986**, *123*(3–4), 115.

[27] Billes, F.; Böhlig, H.; Ackermann, M.; Kudra, M. *J. Mol. Struct.-THEOCHEM* **2004**, *672*, 1.
[28] Kupka, T.; Wrazalik, R.; Pasterna, G.; Pasterny, K. *J. Mol. Struct.* **2002**, *616*, 17.
[29] Furer, V. L.; Borisoglebskaya, E. I.; Zverev, V. V.; Kovalenko, V. I. *Spectrochim. Acta. A.* **2005**, *62*(1–3), 483.
[30] Draeger, J. A. *Spectrochim. Acta. A.* **1983**, *39*(9), 809.
[31] Schrader, B. *Raman/Infrared Atlas of organic Compounds*; 2nd ed., VCH: Weinheim, 1989.
[32] Vicens, J. unpublished results.
[33] Stewart, J. E. *Appl. Optics* **1962**, *1*, 75.
[34] Hall, P. G.; Lovell, V. M.; Finkelstein, N. P. *Trans. Faraday Soc.* **1970**, *66*(570), 1520.
[35] Keresztury, G. *Raman Spectroscopy in Theory in Handbook of Vibrational Spectroscopy*; Chalmers, J. M., Griffiths, P. R., Eds.; John Wiley & Sons, Ltd. Chirchester, 2002; 1, p 71.
[36] Samson, I. M.; Walker, R. T. *The Canadian Mineralogist* **2000**, *38*, 35.
[37] Li, R.; Jiang, Z.; Shi, S.; Yang, H. *J. Mol. Struct.* **2003**, *645*(1), 69.
[38] Winnett, W. K.; Nash, C. P. *Appl. Spectrosc.* **1988**, *42*, 60.